

Article

Development of a Coelenterazine Derivative with Enhanced Superoxide Anion-Triggered Chemiluminescence in Aqueous Solution

José Pedro Silva ¹, Patricia González-Berdullas ¹ , Joaquim C. G. Esteves da Silva ^{1,2} 
and Luís Pinto da Silva ^{1,2,*} 

- ¹ Chemistry Research Unit (CIQUP), Institute of Molecular Sciences (IMS), Faculty of Sciences, University of Porto (FCUP), Rua do Campo Alegre 687, 4169-007 Porto, Portugal; up201705721@edu.fc.up.pt (J.P.S.); patricia.berdullas@fc.up.pt (P.G.-B.); jcsilva@fc.up.pt (J.C.G.E.d.S.)
- ² LACOMEPHI, GreenUPorto, Department of Geosciences, Environment and Territorial Planning, Faculty of Sciences, University of Porto (FCUP), Rua do Campo Alegre 687, 4169-007 Porto, Portugal
- * Correspondence: luis.silva@fc.up.pt

Abstract: Superoxide anion is a reactive oxygen species (ROS) of biological interest. More specifically, it plays a role in intra- and intercellular signaling, besides being associated with conditions such as inflammation and cancer. Given this, efforts have been made by the research community to devise new sensing strategies for this ROS species. Among them, the chemiluminescent reaction of marine Coelenterazine has been employed as a sensitive and dynamic probing approach. Nevertheless, chemiluminescent reactions are typically associated with lower emissions in aqueous solutions. Herein, here we report the synthesis of a new Coelenterazine derivative with the potential for superoxide anion sensing. Namely, this novel compound is capable of chemiluminescence in a dose-dependent manner when triggered by this ROS species. More importantly, the light-emission intensities provided by this derivative were relevantly enhanced (intensities 2.13×10^1 to 1.11×10^4 times higher) in aqueous solutions at different pH conditions when compared to native Coelenterazine. The half-life of the chemiluminescent signal is also greatly increased for the derivative. Thus, a new chemiluminescence molecule with significant potential for superoxide anion sensing was discovered and reported for the first time.

Keywords: chemiluminescence; coelenterazine; superoxide anion; luminescence; imidazopyrazinones; reactive oxygen species



Citation: Silva, J.P.; González-Berdullas, P.; Esteves da Silva, J.C.G.; Pinto da Silva, L. Development of a Coelenterazine Derivative with Enhanced Superoxide Anion-Triggered Chemiluminescence in Aqueous Solution. *Chemosensors* **2022**, *10*, 174. <https://doi.org/10.3390/chemosensors10050174>

Academic Editor: Maria Ramos-Payan

Received: 12 April 2022

Accepted: 29 April 2022

Published: 5 May 2022

Publisher's Note: MDPI stays neutral with regard to jurisdictional claims in published maps and institutional affiliations.



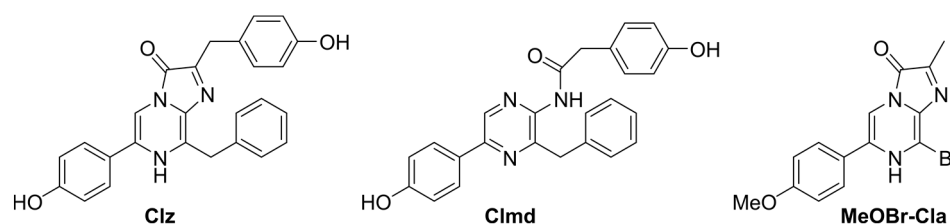
Copyright: © 2022 by the authors. Licensee MDPI, Basel, Switzerland. This article is an open access article distributed under the terms and conditions of the Creative Commons Attribution (CC BY) license (<https://creativecommons.org/licenses/by/4.0/>).

1. Introduction

Chemiluminescence (CL) is the conversion of thermal energy into excitation energy, leading to the emission of visible light due to a chemical reaction [1,2]. Bioluminescence can be considered as a sub-type of CL related to living organisms and catalyzed by an enzyme [1,2]. Typically, CL reactions involve the formation of a peroxide-based high-energy intermediate, the subsequent exothermic decomposition of which allows for direct chemiexcitation into singlet excited states [2–5].

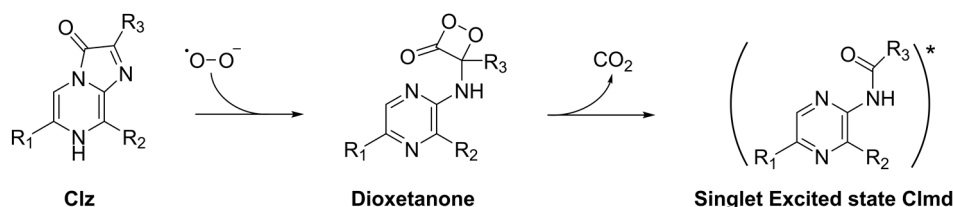
One of the most remarkable properties of both CL and BL reactions is that, since they do not require photoexcitation to generate the light-emitter, they present a diminished probability of autofluorescence arising from a background signal (increasing the signal-to-noise ratio) [6,7] and thus allow for the generation of luminescent signals with high sensitivity and almost no background noise [8], which can be particularly useful for applications in biologic media. In fact, both CL and BL have been gaining practical applications in fields as different as real-time imaging [9–11] and cancer therapy [12–14]. Nevertheless, the most widespread use of CL and BL substrates/reactions is arguably in sensing applications [15–20].

Among existent CL/BL substrates, Coelenterazine (Clz, Scheme 1) is one of the most well-known and studied [1,2,21–26]. Around 80% of all bioluminescent organisms are present in the oceans and the majority of them employ Clz and other related imidazopyrazinones as BL substrates [27]. Clz itself is capable both of BL (in the presence of either luciferase enzymes or photoproteins) [2] and CL (triggered by oxygenation without an enzyme/photoprotein) [28–30]. The CL and BL reactions of Clz generally follow a two-step mechanism [1,2,12–14,21–30]: there is an oxygenation of the imidazopyrazinone core leading to the formation of the high-energy peroxide intermediate, dioxetanone, which is quite unstable and undergoes thermolysis almost instantly. During this decomposition, the reacting molecules can cross directly to singlet excited states, thereby generating the chemiexcited light-emitter Coelenteramide (Clmd, Scheme 1).



Scheme 1. Structures of Clz, Clmd, and MeOBr-Cla.

Interestingly, Clz can undergo CL in aqueous solutions in the presence of superoxide anion (Scheme 2) [31]. Superoxide anion acts as a trigger of the CL reaction, enabling the oxygenation step, thereby generating the dioxetanone intermediate and subsequently the chemiexcited Clmd chemiluminophore. This feature of the Clz system is quite interesting due to the biological roles that the superoxide anion can play. Namely, the superoxide anion and other reactive oxygen species (ROS) are involved in intra- and intercellular signaling pathways, affecting several cellular events such as cell proliferation and apoptosis [32]. Furthermore, while the quantity of superoxide anion and other ROS is typically regulated by the enzymatic machinery of cells, an unbalance can lead to deleterious health conditions such as inflammation and cancer [33]. This loss of the enzymatic ability to produce superoxide anion could also lead to chronic granulomatous disease [34]. Given this, it is not surprising that different authors have been trying to utilize Clz and derivatives as CL-based chemosensors for superoxide anion determination in general, and in biological media specifically [29,35–37]. These studies have then validated the use of Clz as a reliable approach for the sensitive and dynamic sensing of superoxide anion [29]. However, CL reactions tend to possess lower light-emitting intensities in aqueous solution due to energy loss to water molecules [38,39], and Clz is not an exception [28]. Thus, superoxide anion sensing would benefit from Clz-based CL reactions with enhanced emission in aqueous solutions.



Scheme 2. Schematic representation of the superoxide anion-induced CL reaction of Clz and derivatives. *: the standard symbol to indicate that a compound is in an excited state.

In recent years, our group has been focused on providing new properties and features to the CL system of Clz [12,13]. More specifically, we have developed different Clz analogs (Cla compounds) that showed tumor-selective anticancer activity when triggered by superoxide anion. Based on this experience, here we report a novel Cla compound, MeOBr-Cla (Scheme 1), in which the phenol group of Clz is replaced by a methoxyphenyl moiety, the *p*-cresol by a hydrogen atom, and the benzyl group by a bromine heteroatom. This compound was shown to be able to undergo CL when triggered by superoxide anion

in aqueous solution while showing significantly enhanced emission in comparison with Clz. Thus, this novel derivative shows the potential to be considered a prototypical system for the enhanced sensing of superoxide anion by CL methodologies.

2. Materials and Methods

2.1. Synthesis

The synthesis of MeOBr-Cla was performed by employing synthetic routes already validated by our team [12,13]. The description of the followed procedures can be found in detail in the Supporting Information. Shortly, the synthesis started with a Suzuki–Miyaura cross-coupling reaction between commercial 5-bromopyrazin-2-amine and (4-methoxyphenyl)boronic acid in the presence of K_2CO_3 , to generate the intermediate 5-(4-methoxyphenyl)pyrazin-2-amine (MeO-Clm). The bromination of MeO-Clm was performed by the addition of *N*-bromosuccinimide in ethanol to yield 3-bromo-5-(4-methoxyphenyl)pyrazin-2-amine (MeOBr-Clm). Finally, the formation of the imidazopyrazinone core is achieved upon the reaction of MeOBr-Clm with methylglyoxal in acid media to yield MeOBr-Cla. The structural characterization of MeO-Clm, MeOBr-Clm, and MeOBr-Cla was performed by 1H and ^{13}C NMR spectroscopy (Figures S1–S3) and FT-MS spectrometry (Figures S4–S6).

2.2. Luminometric and Spectroscopy Characterization

UV-Vis spectroscopy assays were performed at room temperature in a VWR® UV-Vis Spectrophotometer (UV-3100PC) with a quartz cuvette. Fluorescence spectra were measured with a Horiba Jovin Fluoromax 4 spectrofluorometer, with an integration time of 0.1 s. Slit widths of 5 nm were used for both the excitation and emission monochromators. CL spectra were obtained with the same spectrofluorometer but with a slit of 29 nm for the emission monochromators. Quartz cuvettes were used for both fluorescence and CL spectra. CL kinetic measurements were performed in a homemade luminometer using a Hamamatsu JC135-01 photomultiplier tube. All reactions took place at room temperature at least in sextuplicate. The light was integrated and recorded in 0.1 s intervals. Typical CL assays were measured for 4 min after the initial burst of light.

3. Results and Discussion

3.1. Chemistry of MeOBr-Cla

MeOBr-Cla (Scheme 1) was synthesized with methodologies already validated and optimized by our team [12,13]. In short (details in Supporting Information), it consisted of an initial Suzuki–Miyaura cross-coupling between commercial 5-bromopyrazin-2-amine and an appropriated phenylboronic acid to yield the first intermediate. Subsequently, a bromine heteroatom was introduced near the amine group, followed by cyclization with methylglyoxal to yield MeOBr-Cla. The structures of MeOBr-Cla and synthesis intermediates were confirmed with both $^1H/^{13}C$ NMR and FT-MS spectroscopy (Figures S1–S6).

The absorption spectrum of MeOBr-Cla was obtained in aqueous solution (Figure 1). It consists of sharp absorption in the 200–250 nm range, two main bands at ~275 and ~355 nm, and a shoulder at ~400 nm.

The 2D excitation–emission matrix (EEM) contour plot (Figure 1) for MeOBr-Cla in aqueous solution is also presented in Figure 1. This shows that the fluorescence of this compound consists of two emissive centers with the same emission wavelength maximum (~450 nm) and two different excitation maxima (~275 and ~350 nm). Moreover, the emissive center with the lower excitation wavelength leads to more intense fluorescence than the one with excitation in the UVA region. Given the overlap between absorption and excitation bands (at ~275 and ~350 nm), the different emissive centers are just attributed to excitation from the ground state to different excited states (corresponding to different absorption bands), which are then converted into the same lowest singlet excited state (in accordance with Kasha's rule) [40].

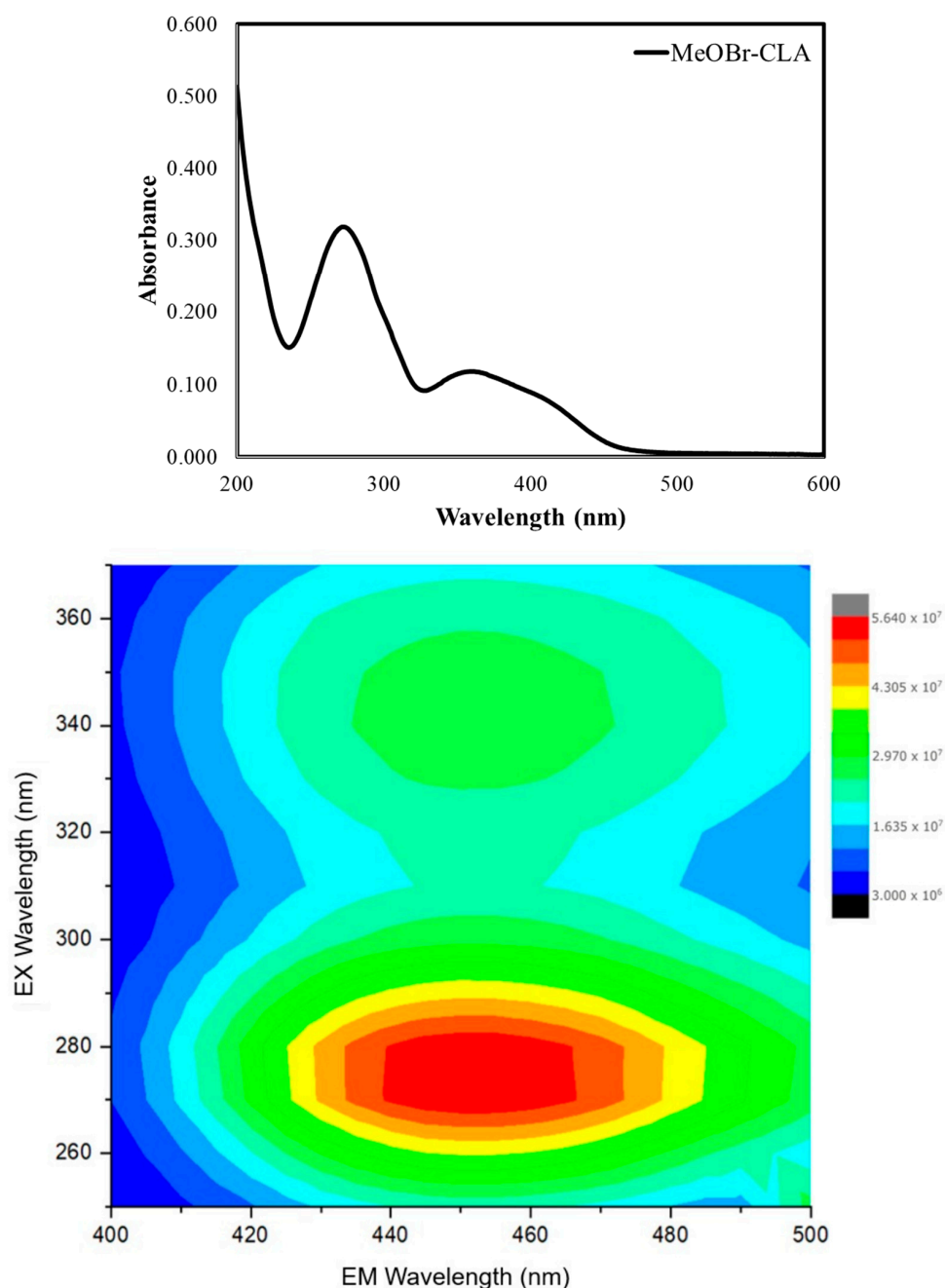


Figure 1. Absorption spectrum (top) and 2D EEM contour plot (bottom) for MeOBr-CLA (30 μ M) in aqueous solution.

3.2. Superoxide Anion-Induced CL of MeOBr-CLA in Aqueous Solution

The next step of this study was then to verify if the superoxide anion could trigger the CL reaction of MeOBr-CLA in aqueous solution. To that end, the CL kinetic profile (light emission as a function of time) of MeOBr-CLA was obtained with a luminometric approach [6,12,13,23,24,28,41–44] in the presence of potassium superoxide. This compound is a typical source of superoxide anion in protic solvents in the study of Clz/CLA-based CL reactions [12,13,45,46]. Measurements were performed in acidic, neutral, and basic pH, in typical conditions used in previous CL-based studies [6,12,13,28,41–44,47,48]. Namely, measurements in acidic pH were performed by the addition of sodium acetate buffer pH 5.2 (1%), in neutral pH by the addition of phosphate buffer pH 7.4 (75 mM), and in basic pH by the addition of NaOH (0.1 M). pH values indicated regarding buffers correspond to the pH of the commercial buffer solutions (sodium acetate pH 5.2 and

phosphate buffer pH 7.4). Measurements were also performed with increasing amounts of potassium superoxide (5, 10, and 15 mg) [12,13].

The representative and normalized CL kinetic profiles of MeOBr-Clz in aqueous solutions of different pH, and in the presence of 10 mg of potassium superoxide, can be found in Figure 2. These kinetic measurements also gave rise to the light-emission maxima (in relative light units, RLU), calculated area (light emission as a function of time, in RLU), and initial velocities of the CL reaction (in RLU/seconds, RLU/s). Initial velocities are obtained by the increase in light production over the first milliseconds after the start of the reaction in the linear range of the CL profile [49,50]. These values are presented in Table 1.

Table 1. Light-emission intensity maxima (in RLU), area of emitted light (in RLU), and initial velocities (in RLU/s) of the CL reactions of MeOBr-Clz in aqueous solutions with the addition of either sodium acetate buffer pH 5.2 (1%), phosphate buffer pH 7.4 (75 mM), or NaOH (0.1 M). Measurements were performed with different amounts of potassium superoxide (5–15 mg) as the superoxide anion source. Assays were performed for a final volume of 500 μ L and a MeOBr-Clz concentration of 5 μ M.

Potassium Superoxide (mg)	Emission Intensity (RLU)	Emission Area (RLU)	Initial Velocity (RLU/s)
Acetate Buffer pH 5.2			
5	$2.38 \times 10^6 \pm 1.30 \times 10^5$	$8.15 \times 10^6 \pm 2.54 \times 10^6$	$8.83 \times 10^6 \pm 1.42 \times 10^6$
10	$2.05 \times 10^6 \pm 3.92 \times 10^4$	$4.00 \times 10^6 \pm 2.38 \times 10^5$	$8.08 \times 10^6 \pm 8.71 \times 10^5$
15	$1.72 \times 10^6 \pm 6.99 \times 10^4$	$2.20 \times 10^6 \pm 1.75 \times 10^5$	$6.61 \times 10^6 \pm 8.26 \times 10^5$
Phosphate Buffer pH 7.4			
5	$9.87 \times 10^5 \pm 9.00 \times 10^4$	$1.89 \times 10^6 \pm 1.64 \times 10^5$	$2.61 \times 10^6 \pm 3.24 \times 10^5$
10	$5.64 \times 10^5 \pm 2.97 \times 10^4$	$1.02 \times 10^6 \pm 1.25 \times 10^5$	$1.81 \times 10^6 \pm 2.30 \times 10^5$
15	$7.69 \times 10^5 \pm 4.16 \times 10^4$	$1.25 \times 10^6 \pm 5.39 \times 10^4$	$1.71 \times 10^6 \pm 3.42 \times 10^5$
NaOH 0.1 M			
5	$5.39 \times 10^3 \pm 3.05 \times 10^2$	$9.69 \times 10^5 \pm 8.55 \times 10^4$	$4.38 \times 10^3 \pm 4.41 \times 10^2$
10	$3.76 \times 10^3 \pm 1.17 \times 10^2$	$5.77 \times 10^5 \pm 4.32 \times 10^4$	$7.29 \times 10^3 \pm 5.76 \times 10^2$
15	$3.59 \times 10^3 \pm 1.00 \times 10^2$	$4.45 \times 10^5 \pm 7.88 \times 10^3$	$7.71 \times 10^3 \pm 5.23 \times 10^2$

The CL kinetic profiles of MeOBr-Clz in aqueous solutions show that superoxide anion does trigger the CL reaction of this Clz derivative (Figure 2). In terms of the shape of the kinetic profile, there do not appear to exist relevant differences at acidic and neutral pH, as in these conditions there is an initial burst of light with rapid decay to basal levels. Nevertheless, this is somewhat different for basic pH, as after reaching the emission maximum, the light intensity decreases but reaches a plateau not so much lower than the emission maximum. There were also relevant quantitative differences regarding all conditions.

An analysis of Table 1 shows that the total light output of the CL reaction of MeOBr-Clz is significantly greater at lower pH values. In fact, in terms of light-emission maxima, MeOBr-Clz produces two to four times more light in acetate buffer than in phosphate buffer or NaOH (respectively), at lower amounts of potassium superoxide. Regarding the calculated area of light emission, differences are even more significant, with MeOBr-Clz generating four to eight times more total light in acidic media than in either neutral or basic conditions (respectively). Initial velocities are also higher in acidic media. This data indicates that the efficiency of the superoxide anion–CL reaction of MeOBr-Clz is pH-dependent, which is not surprising, as this is a common feature of the CL reaction of Clz and derivatives [6,12,13,24,41–44,47–50]. This has been attributed to the chemical equilibria of dioxetanone (Scheme 1). Namely, the chemiexcitation pathway of neutral dioxetanone (protonated amide group) has been found to be more efficient than that of anionic dioxetanone (deprotonated amide group), with the former being more present in acidic media and the latter at higher pH values [6,12,13,24,41–44,47–50]. Other factors could also be at play here. For instance, the lower light emission at higher pH and its

different kinetic profile (continuous but low emission) could point to the interaction of this derivative with superoxide anion being less efficient than at lower pH values. At basic pH, it should be expected that the imidazopyrazinone core becomes ionized (with the deprotonation of the NH group) [12], which should impair its interaction with the also negatively charged superoxide anion.

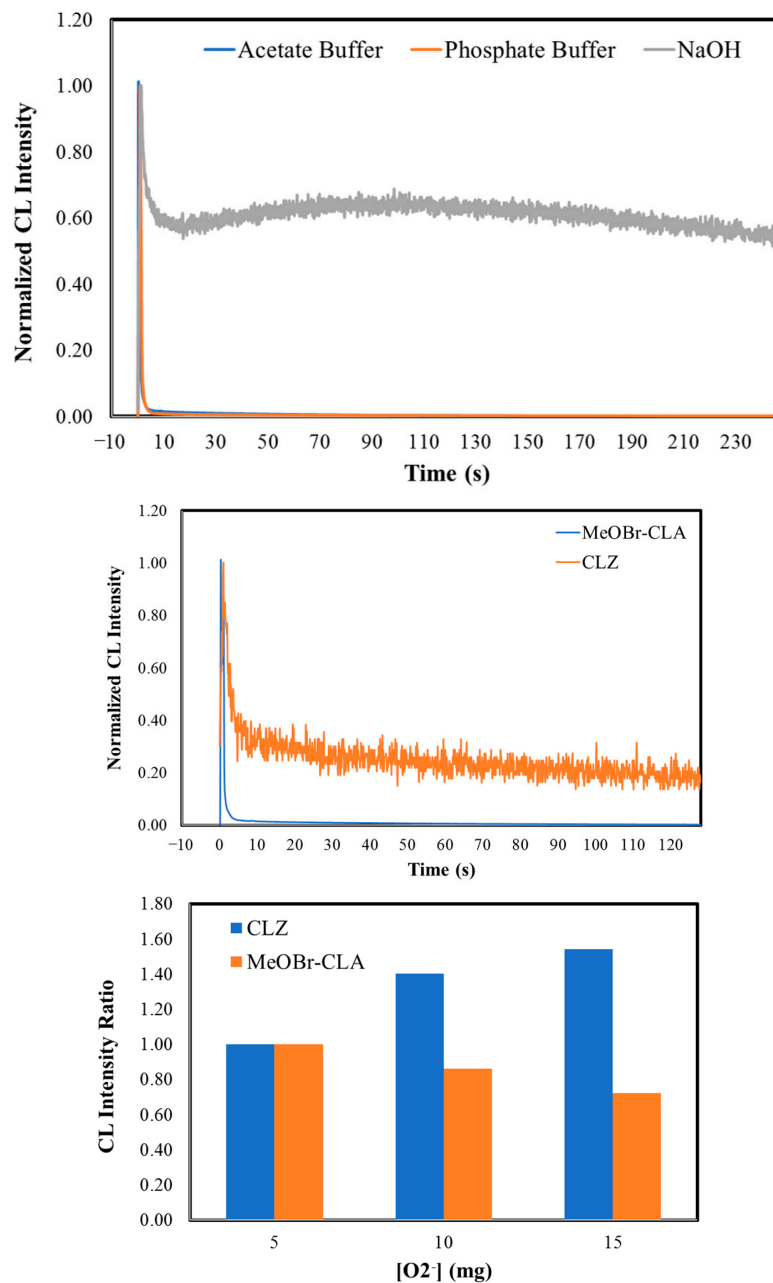


Figure 2. Normalized CL kinetic profiles for MeOBr-Clz in aqueous solutions with the addition of either sodium acetate buffer pH 5.2 (1%), phosphate buffer pH 7.4 (75 mM), or NaOH (0.1 M), in the presence of 10 mg of potassium superoxide (top). Normalized CL kinetic profiles for both MeOBr-Clz and Clz in aqueous solution with the addition of phosphate buffer pH 7.4 (75 mM), in the presence of 10 mg of potassium superoxide (middle). CL intensity ratios for the CL reactions of both Clz and MeOBr-Clz in aqueous solutions with the addition of sodium acetate buffer pH 5.2 (1%), in the presence of increasing amounts of potassium superoxide (5 to 15 mg). The CL intensities obtained for each molecule in the presence of 5 mg of potassium superoxide were used as a reference for Clz and MeOBr-Clz (bottom). All assays were performed for a final volume of 500 μ L and a concentration of 5 μ M of Clz/MeOBr-Clz.

Further analysis of Table 1 also reveals that the CL reaction is sensitive to the amount of superoxide anion. More specifically, increasing amounts of potassium superoxide decrease the total light output of the CL reaction of MeOBr-Cl_a. This decrease is found for all pH conditions, meaning that this is an intrinsic feature of this system, not subjected to the different ionization states of the involved molecules. In terms of light-emission maxima, decreases of 28, 22, and 33% are observed for acidic, neutral, and basic media and potassium superoxide amounts ranging between 5 and 15 mg. For the calculated area, the decreases are 73, 34, and 54%, respectively.

Given this, these results indicate that the CL reaction of MeOBr-Cl_a can be triggered by superoxide anion in aqueous solution and that the reaction is sensitive to the amount of this particular ROS species. Thus, and based on previous research on this class of imidazopyrazinonic compounds [29,35–37], this molecule shows potential for future uses and development as a CL probe for superoxide anion. Furthermore, given the pH-dependency of the CL reaction of MeOBr-Cl_a, it also shows potential as a probe for the simultaneous sensing of both pH and superoxide anion, which could be particularly useful for certain biological conditions/processes. For example, cancer cells are typically associated with both the overexpression of superoxide anion [33] and a lower pH than normal cells [51], so the simultaneous determination of both parameters is desired.

Nevertheless, to fully determine the potential of MeOBr-Cl_a to respond to superoxide anion, we must first compare its CL performance to that of native Cl_z. To that end, we also measured the CL kinetic profiles of Cl_z in aqueous solution with the addition of either sodium acetate buffer pH 5.2 (1%), phosphate buffer pH 7.4 (75 mM), or NaOH (0.1 M), in the presence of increasing amounts of potassium superoxide (5, 10, and 15 mg). The kinetic profile of Cl_z (at phosphate buffer pH 7.4 in the presence of 10 mg of potassium superoxide) is compared with that of MeOBr-Cl_a in the same conditions in Figure 2. The CL kinetic profile of Cl_z is quite identical to that of MeOBr-Cl_a at the same conditions, with both compounds following a flash-type profile with a quick burst of light followed shortly by decay to basal levels.

A quantitative comparison between compounds was also performed by calculating the ratios ($\frac{MeOBr-Cl_a}{Cl_z}$) between MeOBr-Cl_a and Cl_z for obtained light-emission maxima and calculated areas of light-emission are presented in Table 2. Remarkable differences were obtained with ratios of light-emission maxima and calculated areas of light-emission of 2.13×10^1 – 1.11×10^4 and 8.05×10^1 – 3.16×10^3 , respectively, at different conditions. These values show that the superoxide anion-induced CL of MeOBr-Cl_a is remarkably enhanced in aqueous solution when compared to that of native Cl_z. Given that Cl_z itself has already been validated as a CL probe for this ROS species [29,35–37], this greatly enhanced emission indicates that MeOBr-Cl_a presents significant potential to be used in the future as a CL probe in biological media.

Further analysis of Table 2 indicates that the $\frac{MeOBr-Cl_a}{Cl_z}$ ratio generally decreases with increasing amounts of potassium superoxide. To further evaluate if this results from MeOBr-Cl_a and Cl_z presenting the same response toward superoxide, we plotted the CL light-emission intensity maxima of these compounds as a function of the amount of potassium superoxide (Figure 2) in aqueous solution with the addition of sodium acetate buffer pH 5.20 (1%). CL intensities were presented as ratios, with the CL light-emission intensity maxima for each compound in the presence of 5 mg of potassium superoxide used as the reference. These results indicate that Cl_z and MeOBr-Cl_a present opposite responses toward superoxide anion, with increasing amounts of this ROS leading to more/less CL emission for the two compounds (respectively). Though superoxide anion leads to increasing CL emission for Cl_z, it should be noted that its emission in the presence of 15 mg of potassium superoxide is still significantly less intense than that of MeOBr-Cl_a in the same conditions (ratio of 5.18×10^3 , Table 2), which demonstrates the significant enhancement of MeOBr-Cl_a and its high potential for superoxide anion sensing. Given the fact that increasing amounts of superoxide anion led to decreasing intensities of MeOBr-Cl_a, it can be hypothesized that this results from this ROS role as a moderate oxidant. Thus,

it is possible that MeOBr-Cla could be more sensitive to over-oxidation by superoxide anion than Clz, meaning that increasing amounts of superoxide anion lead not only to CL emission but to the over-oxidation of this compound. Nevertheless, since the CL emission of MeOBr-Cla is sensitive to variations in the amount of superoxide anion, it should be possible to obtain correlations between the analytical signal and the concentration of the analyte.

Table 2. Measured ratios between the obtained light-emission maxima and calculated area of the CL reactions of MeOBr-Cla and Clz ($\frac{\text{MeOBr-Cla}}{\text{Clz}}$). Measurements were performed in aqueous solutions with the addition of either sodium acetate buffer pH 5.2 (1%), phosphate buffer pH 7.4 (75 mM), or NaOH (0.1 M). Measurements were performed with different amounts of potassium superoxide (5–15 mg), as a superoxide anion source. Assays were performed for a final volume of 500 μL and a concentration of 5 μM for both Clz and MeOBr-Cla.

Superoxide [O_2^-] (mg)	Emission Intensity	Emission Area
Acetate Buffer pH 5.2		
5	$1.11 \times 10^4 \pm 2.31 \times 10^3$	$3.16 \times 10^3 \pm 1.42 \times 10^3$
10	$6.80 \times 10^3 \pm 5.10 \times 10^2$	$1.04 \times 10^3 \pm 1.53 \times 10^2$
15	$5.18 \times 10^3 \pm 5.57 \times 10^2$	$3.96 \times 10^2 \pm 7.03 \times 10^1$
Phosphate Buffer pH 7.4		
5	$6.62 \times 10^2 \pm 1.12 \times 10^2$	$1.49 \times 10^2 \pm 3.04 \times 10^1$
10	$2.45 \times 10^2 \pm 2.54 \times 10^1$	$1.11 \times 10^2 \pm 2.72 \times 10^1$
15	$1.29 \times 10^2 \pm 2.72 \times 10^1$	$5.30 \times 10^1 \pm 5.25 \times 10^0$
NaOH 0.1 M		
5	$2.53 \times 10^1 \pm 5.91 \times 10^0$	$9.43 \times 10^1 \pm 2.77 \times 10^1$
10	$2.13 \times 10^1 \pm 3.39 \times 10^0$	$9.81 \times 10^1 \pm 1.73 \times 10^1$
15	$2.46 \times 10^1 \pm 3.26 \times 10^0$	$8.05 \times 10^1 \pm 1.24 \times 10^1$

3.3. CL of MeOBr-Cla in Aprotic Solvents

Having demonstrated that MeOBr-Cla presents a remarkably enhanced CL emission when triggered by superoxide anion when compared to a known probe for this ROS species (Clz) [29,35–37], it is important to further characterize the intrinsic properties of this new CL substrate. More specifically, it should be noted that superoxide anion can be quite unstable in protic media, especially in aqueous solution, due to strong solvation and spontaneous disproportionation [52,53]. Thus, some of the properties found in the previous section could be more a result of the instability of superoxide anion than due to the CL reaction of MeOBr-Cla. For example, the rather quick flash profile (Figure 2) observed in aqueous solution could be attributed to the instability of the triggering ROS, superoxide anion, instead of to the intrinsic kinetics of the CL reaction of MeOBr-Cla. To address this, we have also studied the CL reaction of MeOBr-Cla in the aprotic solvent *N,N*-dimethylformamide (DMF) in the absence of superoxide anion or any catalyst. CL reactions are known to be triggered spontaneously in aprotic solvents, such as DMF, while showing stable signals [6,12,13,24,41–44,47–50]. Assays were also performed at different pH conditions, with the addition of either sodium acetate buffer pH 5.2 (1%), phosphate buffer pH 7.4 (75 mM), or NaOH (0.1 M) [6,12,13,24,41–44,47–50].

The normalized CL kinetic profiles of MeOBr-Cla in DMF, at different pH conditions, are presented in Figure 3. In fact, we can see that while there is still an initial burst of light reaching a maximum almost instantly, the decay is significantly slower. Interestingly, the qualitative decay of MeOBr-Cla at basic pH is quicker than at acidic and neutral pH, which are similar themselves.

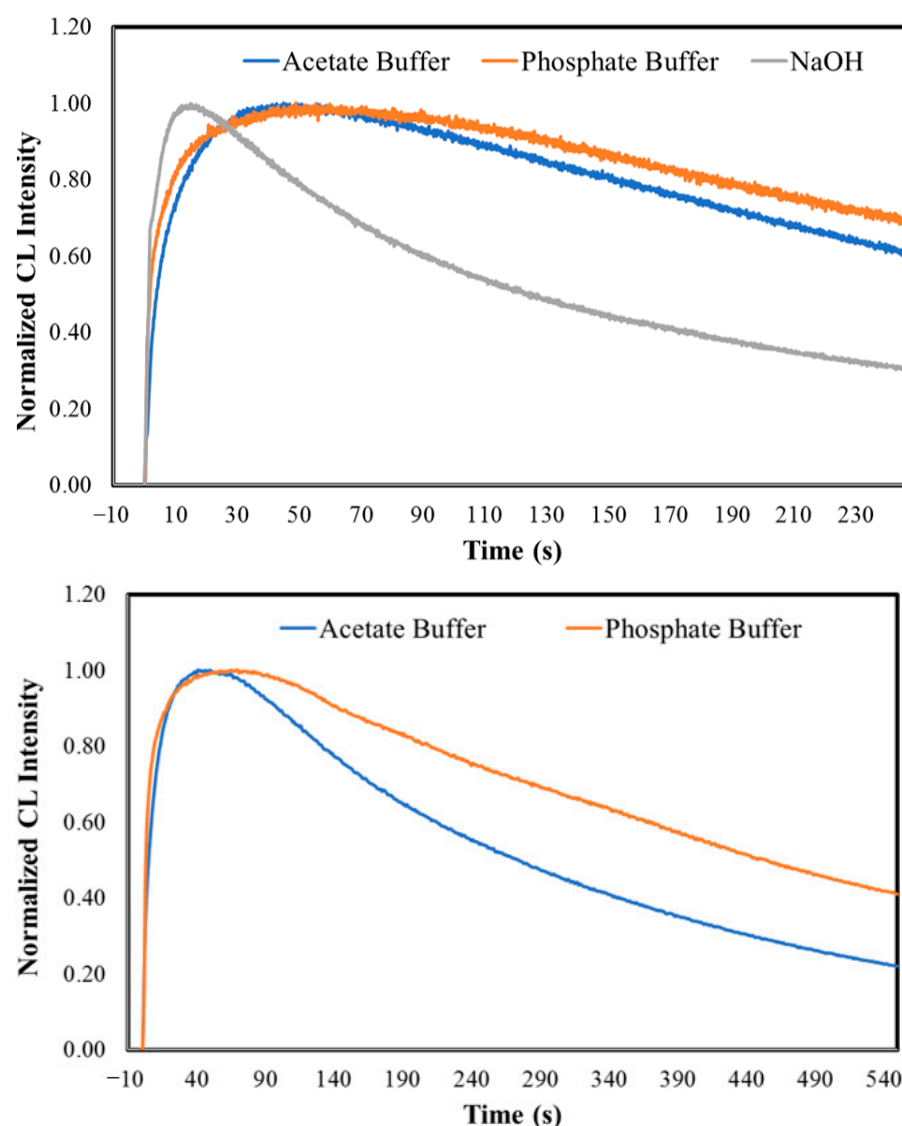


Figure 3. Normalized CL kinetic profiles for MeOBr-ClA in DMF with the addition of either sodium acetate buffer pH 5.2 (1%), phosphate buffer pH 7.4 (75 mM), or NaOH (0.1 M), measured with an integration time of 0.1 s (top). Normalized CL kinetic profiles for MeOBr-ClA in DMF with the addition of either sodium acetate buffer pH 5.2 (1%) or phosphate buffer pH 7.4 (75 mM), with an integration time of 1 s (bottom). All assays were performed with a final volume of 500 μ L and a concentration of 10 μ M of MeOBr-ClA.

Quantitative analysis was performed by measuring the light-emission intensity maxima (in RLU), calculated area of light emission (in RLU), and initial velocities (RLU/s) for CL reactions that occurred in DMF at different pH conditions (Table 3). Given the longer decay times, we were also able to determine CL half-life values (in s), also shown in Table 3.

In general, it does seem that light-emission maxima and initial velocities increase with increasing pH, while the calculated area decreases (Table 3). This indicates that the kinetics of the CL reaction at basic pH are significantly quicker, leading to a faster initial burst of light. However, that does not mean that MeOBr-ClA produces more light at basic pH. The fact that the calculated area of light emission is higher at acidic pH indicates that the total light output is higher but also released during a larger period. Once again, this can be explained at least partly due to the chemical equilibria associated with the dioxetanone intermediate (Scheme 1) [6,12,13,24,41–44,47–50].

The half-time value of the CL reaction in DMF with the addition of NaOH (0.1 M) was 107.05 ± 14.70 s (Table 3). Interestingly, the typical measurement times (4 min with an

integration time of 0.1 s) were not enough to allow for the determination of half-life values in DMF with the addition of either sodium acetate buffer pH 5.2 (1%) or phosphate buffer pH 7.4 (75 mM). Thus, the half-life for the CL reactions at these conditions was calculated by measurements for longer periods (15 min) and an integration time of 1 s (Figure 3 and Table 3). The half-life values are relevantly higher at acidic and neutral pH; nevertheless, the pH should not be the sole determining factor, as the half-life for neutral pH (546 ± 90 s) is relevantly higher than for acidic pH (251 ± 5 s). Thus, further exploration of this topic should be pursued in the future.

Table 3. Light-emission intensity maxima (in RLU), area of emitted light (in RLU), initial velocities (in RLU/s), and half-life(s) of the CL reactions of MeOBr-Cla in DMF with the addition of either sodium acetate buffer pH 5.2 (1%), phosphate buffer pH 7.4 (75 mM), or NaOH (0.1 M). Assays were performed for a final volume of 500 μ L and a MeOBr-Cla concentration of 10 μ M. Typical integration times for CL measurements were 0.1 s.

Solvent	Emission Intensity (RLU)	Emission Area (RLU)	Initial Velocity (RLU/s)	Half-Life (ms)
DMF + Acetate Buffer pH 5.2	$4.77 \times 10^4 \pm 2.68 \times 10^3$	$9.98 \times 10^6 \pm 5.53 \times 10^5$	$9.92 \times 10^3 \pm 1.77 \times 10^3$	$251^a \pm 5$
DMF + Phosphate Buffer pH 7.4	$3.23 \times 10^4 \pm 2.15 \times 10^3$	$7.14 \times 10^6 \pm 4.61 \times 10^5$	$2.70 \times 10^4 \pm 7.33 \times 10^3$	$546^a \pm 90$
DMF + NaOH	$5.67 \times 10^4 \pm 7.24 \times 10^3$	$6.85 \times 10^6 \pm 5.75 \times 10^5$	$4.69 \times 10^4 \pm 9.28 \times 10^3$	107.05 ± 14.70

^a Integration time of 1 s.

It should be noted that the CL reactions of native Clz in aprotic solvents have been studied before [41]. While half-life values were not explicitly calculated, it can be seen that light emission intensity decreases to about 50% in less than 60 s. Thus, the half-life values of MeOBr-Cla appear to be relevantly higher than those of Clz. This should also be an attractive feature for the CL reaction of this novel compound, as a longer half-life should facilitate the detection of the analytical signal.

Finally, we have measured the CL spectra of MeOBr-Cla in DMF with the addition of either sodium acetate buffer pH 5.2 (1%) or NaOH (0.1 M), which are shown in Figure 4. The CL spectrum at acidic pH is composed of two somewhat overlapped bands, with emission maxima at \sim 410 and \sim 460 nm. At basic pH, the CL spectrum is just composed of a band at \sim 460 nm. This behavior indicates that the emission of the chemiluminophore (the Clmd version of MeOBr-Cla, Figure 1) is pH-dependent, which is not strange for imidazopyrazinones and can be attributed to the chemical equilibria of the amide group of Clmd (Figure 1) [22,41]. More specifically, at acidic pH, the neutral (emission at \sim 410 nm) and anionic amide species (emission at \sim 460 nm) of the Clmd version of MeOBr-Cla (Figure 1) should coexist, while at basic pH, deprotonation is complete, and only emission from the anionic amide species is observed. In fact, it has been found before that the CL spectra of native Clz in aprotic solvents are composed of one band at acidic pH (\sim 475 nm), while increasing the pH leads to a red-shift in emission to \sim 515 nm, also attributed to the deprotonation of Clmd [41]. So, these results also indicate that the CL emission of MeOBr-Cla is blue-shifted with regard to native Clz.

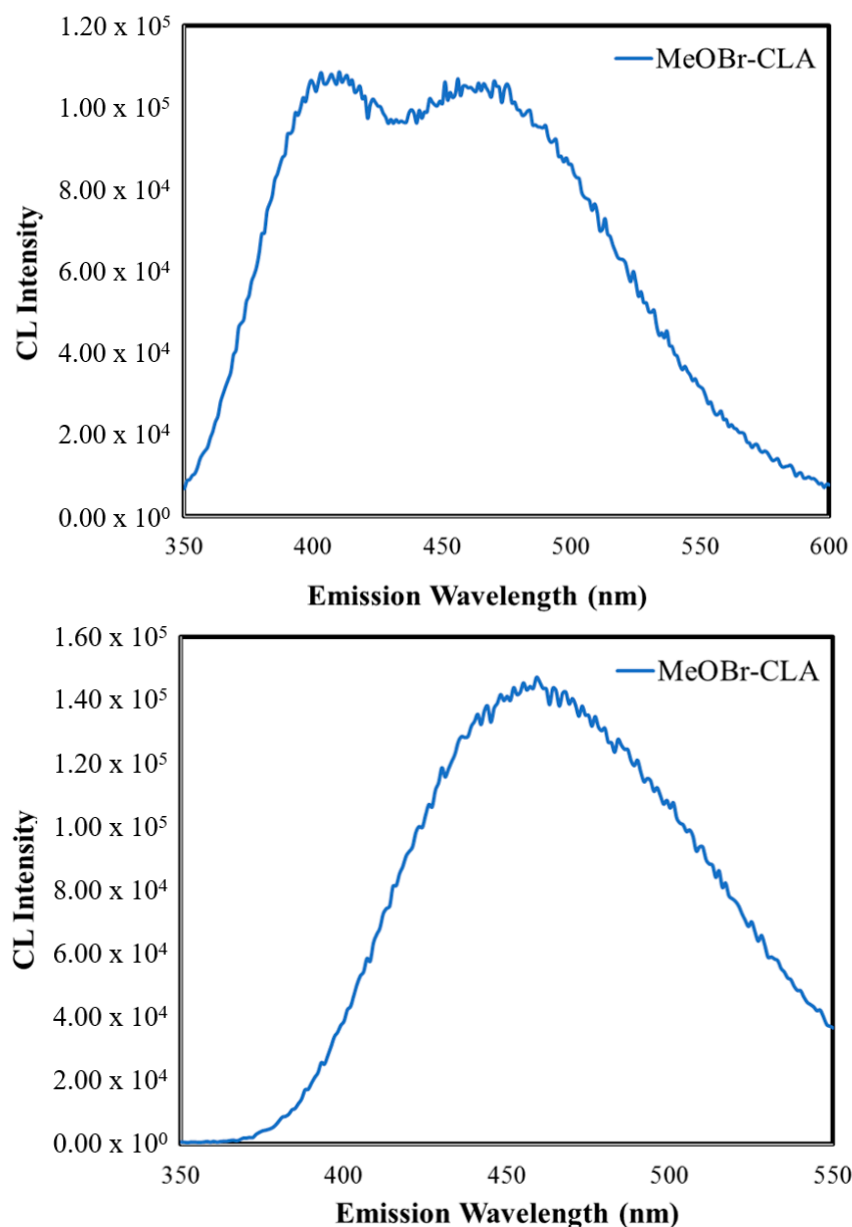


Figure 4. CL spectra for MeOBr-ClA in DMF with the addition of either sodium acetate buffer pH 5.2 (1%) (top) or NaOH (0.1 M) (bottom).

4. Conclusions

Superoxide anion is an ROS species of biological interest that is involved in intra- and intercellular signaling pathways and deleterious conditions, such as inflammation and cancer. Given this, it is important to possess sensitive and dynamic sensing approaches for its determination and imaging. One such approach is the CL reaction of marine Clz.

Here, we described the synthesis of a Clz derivative, MeOBr-ClA, and the characterization of its CL reaction in aqueous solution. This compound showed a dose-dependent CL response to superoxide anion, which resulted in a significant and remarkable light-emission enhancement when compared to native Clz. The half-life of the CL reaction of MeOBr-ClA was also found to be relevantly greater than that of Clz, which should benefit the determination of the analytical signal. The CL reaction of MeOBr-ClA was also found to be responsive to pH, thereby opening the way for the future development of CL probes for the simultaneous determination of pH and superoxide anion, which should be useful in certain scenarios (e.g., cancer).

Thus, a new Clz derivative with significantly enhanced CL in aqueous solution when triggered by superoxide anion was developed, which indicates it could be considered a prototypical system for the future development of CL probes for superoxide anion with enhanced properties.

5. Patents

WO2019211809—Chemiluminescent imidazopyrazinone-based photosensitizers with available singlet and triplet excited states.

Supplementary Materials: The following supporting information can be downloaded at: <https://www.mdpi.com/article/10.3390/chemosensors10050174/s1>, Figure S1: ^1H NMR, DEPT, and ^{13}C NMR spectra of MeO-Clm, Figure S2: ^1H NMR, DEPT, and ^{13}C NMR spectra of MeOBr-Clm, Figure S3: ^1H NMR spectrum of MeOBr-Clm, Figure S4: FT-MS spectrum of MeO-Clm, Figure S5: FT-MS spectrum of MeOBr-Clm, Figure S6: FT-MS spectrum of MeOBr-Clm.

Author Contributions: Conceptualization, L.P.d.S.; investigation, J.P.S. and P.G.-B.; writing—original draft preparation, J.P.S., P.G.-B. and L.P.d.S.; writing—review and editing, L.P.d.S. and J.C.G.E.d.S.; visualization, P.G.-B. and J.P.S.; supervision, L.P.d.S.; project administration, L.P.d.S.; funding acquisition, L.P.d.S. and J.C.G.E.d.S. All authors have read and agreed to the published version of the manuscript.

Funding: “Fundação para a Ciência e Tecnologia” (FCT, Portugal) is acknowledged for funding project PTDC/QUI-QFI/2870/2020, R&D Units CIQUP (UIDB/00081/2020) and GreenUPorto (UIDB/05748/2020), and the Associated Laboratory IMS (LA/P/0056/2020). Luís Pinto da Silva acknowledges funding from FCT under the Scientific Employment Stimulus (CEECIND/01425/2017 | 2021.00768.CEECIND). Patricia González-Berdullas acknowledges funding for her Post-Doc position within the framework of project PTDC/QUI-QFI/2870/2020.

Institutional Review Board Statement: Not applicable.

Informed Consent Statement: Not applicable.

Acknowledgments: The Laboratory of Computational Modeling of Environmental Pollutant-Human Interactions (LACOMEPhi) and the Materials Centre of the University of Porto (CEMUP).

Conflicts of Interest: The authors declare no conflict of interest.

References

1. Magalhães, C.M.; Esteves da Silva, J.C.G.; Pinto da Silva, L. Chemiluminescence and Bioluminescence as an Excitation Source in the Photodynamic Therapy of Cancer: A Critical Review. *Chem. Phys. Chem.* **2016**, *17*, 2286–2294. [[CrossRef](#)]
2. Vacher, M.; Galván, I.F.; Ding, B.W.; Schramm, S.; Berraud-Pache, R.; Naumov, P.; Ferré, N.; Liu, Y.J.; Navizet, I.; Roca-Sanjuán, D.; et al. Chemi- and bioluminescence of cyclic peroxides. *Chem. Rev.* **2018**, *118*, 6927–6974. [[CrossRef](#)] [[PubMed](#)]
3. Pinto da Silva, L.; Magalhães, C.M.; Esteves da Silva, J.C.G. Interstate Crossing-Induced Chemiexcitation Mechanism as the Basis for Imidazopyrazinone Bioluminescence. *ChemistrySelect* **2016**, *1*, 3343–3356. [[CrossRef](#)]
4. Boaro, A.; Reis, R.A.; Silva, C.S.; Melo, D.U.; Pinto, A.G.G.C.; Bartoloni, F.H. Evidence for the Formation of 1,2-Dioxetane as a High-Energy Intermediate and Possible Chemiexcitation Pathways in the Chemiluminescence of Lophine Peroxides. *J. Org. Chem.* **2021**, *86*, 6633–6647. [[CrossRef](#)] [[PubMed](#)]
5. Schramm, S.; Navizet, I.; Karothu, S.P.; Oesau, P.; Bensmann, V.; Weiss, D.; Beckert, R.; Naumov, P. Mechanistic investigations of the 2-coumarone chemiluminescence. *Phys. Chem. Chem. Phys.* **2017**, *19*, 22852–22859. [[CrossRef](#)] [[PubMed](#)]
6. Pinto da Silva, L.; Pereira, R.F.J.; Magalhães, C.M.; Esteves da Silva, J.C.G. Mechanistic Insight into Cypridina Bioluminescence with a Combined Experimental and Theoretical Chemiluminescent Approach. *J. Phys. Chem. B* **2017**, *121*, 7862–7871. [[CrossRef](#)] [[PubMed](#)]
7. Gnain, S.; Shabat, D. Self-Immolative Chemiluminescence Polymers: Innate Assimilation of Chemiexcitation in a Domino-Like Depolymerization. *J. Am. Chem. Soc.* **2017**, *139*, 10002–10008. [[CrossRef](#)] [[PubMed](#)]
8. Yang, M.; Huang, J.; Fan, J.; Du, J.; Pu, K.; Peng, X. Chemiluminescence for bioimaging and therapeutics: Recent advances and challenges. *Chem. Soc. Rev.* **2020**, *49*, 6800–6815. [[CrossRef](#)]
9. Cronin, M.; Akin, A.R.; Francis, K.P.; Tangney, M. In vivo bioluminescence imaging of intratumoral bacteria. *Methods Mol. Biol.* **2016**, *1409*, 69–77.
10. Grinstead, K.M.; Rowe, L.; Ensor, C.M.; Joel, S.; Daftarian, P.; Dikici, E.; Zingg, J.M.; Daunert, S. Red-Shifted Aequorin Variants Incorporating Non-Canonical Amino Acids: Applications in In Vivo Imaging. *PLoS ONE* **2016**, *11*, e0158579. [[CrossRef](#)]

11. Zhang, Y.; Pang, L.; Ma, C.; Tu, Q.; Zhang, R.; Saeed, E.; Mahmoud, A.E.; Wang, J. Small Molecule-Initiated Light-Activated Semiconducting Polymer Dots: An Integrated Nanoplatfrom for Targeted Photodynamic Therapy and Imaging of Cancer Cells. *Anal. Chem.* **2014**, *86*, 3092–3099. [[CrossRef](#)]
12. Pinto da Silva, L.; Núñez-Montenegro, A.; Magalhães, C.M.; Ferreira, P.J.O.; Duarte, D.; González-Berdullas, P.; Rodríguez-Borges, J.E.; Vale, N.; Esteves da Silva, J.C.G. Single-molecule chemiluminescent photosensitizer for a self-activating and tumor-selective photodynamic therapy of cancer. *Eur. J. Med. Chem.* **2019**, *183*, 111683. [[CrossRef](#)]
13. Pinto da Silva, L.; Magalhães, C.M.; Núñez-Montenegro, A.; Ferreira, P.J.O.; Duarte, D.; Rodríguez-Borges, J.E.; Vale, N.; Esteves da Silva, J.C.G. Study of the Combination of Self-Activating Photodynamic Therapy and Chemotherapy for Cancer Treatment. *Biomolecules* **2019**, *9*, 384. [[CrossRef](#)]
14. Jiang, L.; Bai, H.; Liu, L.; Lv, F.; Ren, X.; Wang, S. Luminescent, Oxygen-Supplying, Hemoglobin-Linked Conjugated Polymer Nanoparticles for Photodynamic Therapy. *Angew. Chem. Int. Ed.* **2019**, *58*, 10660–10665. [[CrossRef](#)]
15. Ye, S.; Hananya, N.; Green, O.; Chen, H.; Zhao, A.Q.; Shen, J.; Shabat, D.; Yang, D. A Highly Selective and Sensitive Chemiluminescent Probe for Real-Time Monitoring of Hydrogen Peroxide in Cells and Animals. *Angew. Chem. Int. Ed.* **2020**, *132*, 14432–14436. [[CrossRef](#)]
16. Shelef, O.; Sedgwick, A.C.; Pozzi, S.; Green, O.; Satchi-Fainaro, R.; Shabat, D.; Sessler, J.L. Turn on chemiluminescence-based probes for monitoring tyrosinase activity in conjunction with biological thiols. *Chem. Commun.* **2021**, *57*, 11386–11389. [[CrossRef](#)]
17. Meier, J.; Hofferber, E.M.; Stapleton, J.A.; Iverson, N.M. Hydrogen Peroxide Sensors for Biomedical Applications. *Chemosensors* **2020**, *7*, 64. [[CrossRef](#)]
18. Berneschi, S.; Trono, C.; Mirasoli, M.; Giannetti, A.; Zangheri, M.; Guardigli, M.; Tombelli, S.; Marchigiani, E.; Baldini, F.; Roda, A. In-Parallel Polar Monitoring of Chemiluminescence Emission Anisotropy at the Solid-Liquid Interface by an Optical Fiber Radial Array. *Chemosensors* **2020**, *8*, 18. [[CrossRef](#)]
19. Ievtukhov, V.; Zadykowicz, B.; Blazheyevskiy, M.Y.; Krzyminski, K. New luminometric method for quantification of biological sulfur nucleophiles with the participation of 9-cyano-10-methylacridinium salt. *Luminescence* **2022**, *37*, 208–219. [[CrossRef](#)]
20. Krzyminski, K.K.; Roshal, A.D.; Rudnicki-Velasquez, P.B.; Zamojc, K. On the use of acridinium indicators for the chemiluminescent determination of the total antioxidant capacity of dietary supplements. *Luminescence* **2019**, *34*, 512–519. [[CrossRef](#)]
21. Min, C.G.; Pinto da Silva, L.; Esteves da Silva, J.C.G.; Yang, X.K.; Huang, S.J.; Ren, A.M.; Zhu, Y.Q. A Computational Investigation of the Equilibrium Constants for the Fluorescent and Chemiluminescent States of Coelenteramide. *Chem. Phys. Chem.* **2017**, *18*, 117–123. [[CrossRef](#)] [[PubMed](#)]
22. Min, C.G.; Ferreira, P.J.O.; Pinto da Silva, L. Theoretically obtained insight into the mechanism and dioxetanone species responsible for the singlet chemiexcitation of Coelenterazine. *J. Photochem. Photobiol. B* **2017**, *174*, 18–26. [[CrossRef](#)] [[PubMed](#)]
23. Ikeda, Y.; Tanaka, M.; Nishihara, R.; Hiruta, Y.; Citterio, D.; Suzuki, K.; Niwa, K. Quantitative evaluation of luminescence intensity from enzymatic luminescence reaction of coelenterazine analogues. *J. Photochem. Photobiol. A* **2020**, *394*, 112459. [[CrossRef](#)]
24. Lindberg, E.; Mizukami, S.; Ibata, K.; Miyawaki, A.; Kikuchi, K. Development of luminescent Coelenterazine derivatives activatable by b-galactosidase for monitoring dual gene expression. *Chem. Eur. J.* **2013**, *19*, 13970–14976. [[CrossRef](#)]
25. Krasitskaya, V.V.; Bashmakova, E.E.; Frank, L.A. Coelenterazine-dependent luciferases as a powerful analytical tool for research and biomedical applications. *Int. J. Mol. Sci.* **2020**, *21*, 7465. [[CrossRef](#)]
26. Jiang, T.; Du, L.; Li, M. Lighting up bioluminescence with coelenterazine: Strategies and applications. *Photochem. Photobiol. Sci.* **2016**, *15*, 466–480. [[CrossRef](#)]
27. Haddock, S.H.D.; Moline, M.A.; Case, J.F. Bioluminescence in the sea. *Annu. Rev. Mar. Sci.* **2010**, *2*, 443–493. [[CrossRef](#)]
28. Lourenço, J.M.; Esteves da Silva, J.C.G.; Pinto da Silva, L. Combined experimental and theoretical study of Coelenterazine chemiluminescence in aqueous solution. *J. Lumin.* **2018**, *194*, 139–145. [[CrossRef](#)]
29. Teranishi, K. Non-invasive and accurate readout of superoxide anion in biological systems by near-infrared light. *Anal. Chim. Acta* **2021**, *1179*, 338827. [[CrossRef](#)]
30. Gagnot, G.; Hervin, V.; Coutant, E.P.; Goyard, S.; Jacob, Y.; Rose, T.; Hibti, F.E.; Quatela, A.; Janin, Y.L. Core-Modified Coelenterazine Luciferin Analogues: Synthesis and Chemiluminescence Properties. *Chem. Eur. J.* **2021**, *27*, 2112–2123. [[CrossRef](#)]
31. Goto, T.; Takagi, T. Chemiluminescence of a Cypridina luciferin analogue, 2-methyl-6-phenyl-3,7-dihydroimidazo(1,2-a)pyrazin-3-one, in the presence of the xanthine-xanthine oxidase system. *Bull. Chem. Soc. Jpn.* **1980**, 833–834. [[CrossRef](#)]
32. Dickinson, B.C.; Chang, C.J. Chemistry and biology of reactive oxygen species in signaling or stress responses. *Nat. Chem. Biol.* **2011**, *7*, 504–511. [[CrossRef](#)]
33. Waris, G.; Ahsan, H. Reactive oxygen species: Role in the development of cancer and various chronic conditions. *J. Carcinog.* **2006**, *6*, 14. [[CrossRef](#)]
34. Arnold, D.E.; Heimall, J.R. A review of chronic granulomatous disease. *Adv. Ther.* **2017**, *34*, 2543–2557. [[CrossRef](#)]
35. Bronsart, L.L.; Stokes, C.; Contag, C.H. Multimodality Imaging of Cancer Superoxide Anion Using the Small Molecule Coelenterazine. *Mol. Imaging Biol.* **2016**, *18*, 166–171. [[CrossRef](#)]
36. Bronsart, L.L.; Stokes, C.; Contag, C.H. Chemiluminescence Imaging of Superoxide Anion Detects Beta-Cell Function and Mass. *PLoS ONE* **2016**, *11*, e0146601. [[CrossRef](#)]
37. Lucas, M.; Solano, F. Coelenterazine is a superoxide anion-sensitive chemiluminescent probe: Its usefulness in the assay of respiratory burst in neutrophils. *Anal. Biochem.* **1992**, *2016*, 273–277. [[CrossRef](#)]

38. Gnaim, S.; Green, O.; Shabat, D. The emergence of aqueous chemiluminescence: New promising class of phenoxy 1,2-dioxetane luminophores. *Chem. Commun.* **2018**, *54*, 2073–2085. [[CrossRef](#)]
39. Green, O.; Eilon, T.; Hananya, N.; Gutkin, S.; Bauer, C.R.; Shabat, D. Opening a Gateway for Chemiluminescence Cell Imaging: Distinctive Methodology for Design of Bright Chemiluminescence Dioxetane Probes. *ACS Cent. Sci.* **2017**, *3*, 349–358. [[CrossRef](#)]
40. Braslavsky, S.E. Glossary of terms used in photochemistry, 3rd edition (IUPAC Recommendations 2006). *Pure Appl. Chem.* **2007**, *79*, 293–465. [[CrossRef](#)]
41. Magalhães, C.M.; Esteves da Silva, J.C.G.; Pinto da Silva, L. Comparative study of the chemiluminescence of coelenterazine, coelenterazine-e and *Cypridina* luciferin with an experimental and theoretical approach. *J. Photochem. Photobiol. B* **2019**, *190*, 21–31. [[CrossRef](#)]
42. Coutant, E.P.; Gagnot, G.; Hervin, V.; Baatallah, R.; Goyard, S.; Jacob, Y.; Rose, T.; Janin, Y.L. Bioluminescence Profiling of NanoKAZ/NanoLuc Luciferase using a chemical library of Coelenterazine Analogues. *Chem. Eur. J.* **2020**, *26*, 948–958. [[CrossRef](#)]
43. Morse, D.; Tannous, B.A. A Water-Soluble Coelenterazine for sensitive in vivo imaging of Coelenterate luciferases. *Mol. Ther.* **2012**, *20*, 692–693. [[CrossRef](#)]
44. Tamaki, S.; Kitada, N.; Kiyama, M.; Fujii, R.; Hirano, T.; Kim, S.B.; Maki, S. Color-tunable bioluminescence imaging portfolio for cell imaging. *Sci. Rep.* **2021**, *11*, 2219. [[CrossRef](#)]
45. Taubert, D.; Breitenbach, T.; Lazar, A.; Censarek, P.; Harlfinger, S.; Berkels, R.; Klaus, W.; Roesen, R. Reaction rate constants of superoxide scavenging by plant antioxidants. *Free Radic. Biol. Med.* **2003**, *35*, 1599–1607. [[CrossRef](#)]
46. Misak, A.; Brezova, V.; Chovanec, M.; Luspai, K.; Nasim, M.J.; Grman, M.; Tomasova, L.; Jacob, C.; Ondrias, K. EPR study of KO₂ as a source of superoxide and BMPO-OH/OOH Radical that cleaves Plasmid DNA and Detects Radical Interaction and H₂S and Se-Derivatives. *Antioxidants* **2021**, *10*, 1286. [[CrossRef](#)]
47. Magalhães, C.M.; Esteves da Silva, J.C.G.; Pinto da Silva, L. Study of coelenterazine luminescence: Electrostatic interactions as the controlling factor for efficient chemiexcitation. *J. Lumin.* **2018**, *199*, 339–347. [[CrossRef](#)]
48. Takahashi, Y.; Kondo, H.; Maki, S.; Niwa, H.; Ikeda, H.; Hirano, T. Chemiluminescence of 6-aryl-2-methylimidazo [1,2-*a*]pyrazin-3(7H)-ones in DMSO/TMG and in diglyme/acetate buffer: Support for the chemiexcitation process to generate the singlet-excited state of neutral oxyluciferin in a high quantum yield in the *Cypridina* (*Vargula*) bioluminescence mechanism. *Tetrahedron Lett.* **2006**, *47*, 6057–6061.
49. Pinto da Silva, L.; Esteves da Silva, J.C.G. Kinetics of inhibition of firefly luciferase by dehydroluciferyl-coenzyme A, dehydroluciferin and l-luciferin. *Photochem. Photobiol. Sci.* **2011**, *10*, 1039–1045. [[CrossRef](#)]
50. Ribeiro, C.; Esteves da Silva, J.C.G. Kinetics of inhibition of firefly luciferase by oxyluciferin and dehydroluciferyl-adenylate. *Photochem. Photobiol. Sci.* **2008**, *7*, 1085–1090. [[CrossRef](#)]
51. Piasentin, N.; Milotti, E.; Chignola, R. The control of acidity in tumor cells: A biophysical model. *Sci. Rep.* **2020**, *10*, 13613. [[CrossRef](#)] [[PubMed](#)]
52. Hayyan, M.; Hashim, M.A.; Al Nashef, I.M. Superoxide ion: Generation and chemical implications. *Chem. Rev.* **2016**, *116*, 3029–3085. [[CrossRef](#)] [[PubMed](#)]
53. Sawyer, D.T.; Valentine, J.S. How super is superoxide? *Acc. Chem. Res.* **1981**, *14*, 393–400. [[CrossRef](#)]